



Phase randomization for spatiotemporal averaging of unwanted interference effects arising from coherence

FERGAL SHEVLIN

Dyoptyka, 7 Westland Court, South Cumberland St., Dublin 2, Ireland (fergal_shevlin@dyoptyka.com)

Received 3 April 2018; revised 17 May 2018; accepted 18 May 2018; posted 18 May 2018 (Doc. ID 327493); published 11 June 2018

An approach to the reduction of unwanted interference effects, such as speckle and inhomogeneity, is to generate sequences of uncorrelated effects over the integration period of the sensor such that they are averaged. A moving diffuser is typically used. An innovative deformable mirror technology is presented as an alternative. Through phase randomization it achieves dynamic divergence of illumination without diffraction losses. It is shown to offer a unique combination of advantages over moving diffusers, including optical efficiency, speed, size, and reliability. Various applications are discussed. © 2018 Optical Society of America

OCIS codes: (140.0140) Lasers and laser optics; (030.6140) Speckle; (120.2040) Displays; (090.2870) Holographic display; (120.3180) Interferometry; (180.0180) Microscopy.

<https://doi.org/10.1364/AO.57.0000E6>

1. INTRODUCTION

Semiconductor diode lasers are available at a variety of wavelengths including the visible, some with optical power >5 W, wall-plug efficiencies $>40\%$, aperture areas <100 μm^2 , and angles of emission <25 deg. Their deployment in optical systems is not straightforward, however, due to interference effects.

A. Speckle

Speckle is a high-contrast, granular pattern that can be seen in Fig. 1 and elsewhere in this paper. It arises when coherent illumination is scattered, for example by a rough surface, and its characteristics are influenced significantly by the parameters of image acquisition; see Fig. 2. It is quantified as the ratio of standard deviation of pixel intensity to mean intensity. Since sensors integrate intensity over space and time, an effective technique for reduction of standard deviation is to generate multiple speckle patterns of equal mean intensity during the integration period. In this case, the speckle contrast ratio is $\sqrt{1/n}$ for n uncorrelated patterns.

When coherent illumination is delivered through an optical system, the maximum possible number of uncorrelated patterns is the ratio of the Airy disc diameter of the sensor optical system to that of the illumination optical system [1]. This imposes a lower limit on the speckle contrast ratio that can be achieved through spatiotemporal averaging.

B. Inhomogeneity

Figure 3 shows irregular distribution of intensity due to interferences arising within the illumination optical system.

Approaches effective for the homogenization of non-coherent illumination, such as light pipes and their lens array equivalents, are not so in this case, as can be inferred from Fig. 4.

C. Moving Diffuser

One means of generating multiple uncorrelated speckle patterns, and of improving homogeneity, is to move a diffuser located in the illumination optical system before any homogenization element. A short surface correlation length is necessary to avoid having to move at impractically high speed. This results in scattering out of the optical system, reducing optical efficiency, even with diffusers of sophisticated designs, such as those shown in Fig. 5. Consequences include reduced optical output power, increased electrical power consumption, and more complex heat management and cooling systems. A convenient means of moving the diffuser at speed is to rotate it. However, problems include the size, reliability, and power consumption of the electro-mechanical system.

2. METHOD

Dyoptyka has developed an innovative phase-randomizing deformable mirror technology for improvement of homogeneity and reduction of speckle and other unwanted interference effects; see Fig. 6. Configurations for different applications and some of its effects are shown in Figs. 7 and 8.

Typical surface deformations are ≤ 1 μm in amplitude, ≥ 100 μm in wavelength, and ≥ 100 kHz in temporal frequency. An electronic actuation, sensing, and closed-loop control system comprising proprietary algorithms, implemented

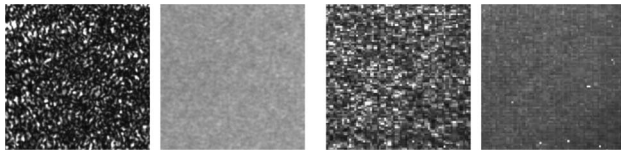


Fig. 1. [Left pair] Semiconductor wafer inspection microscope image with 213 nm (DUV) laser illumination. [Right pair] Thermal infrared sensor calibration system image with 10.6 μm (LWIR) laser illumination. [Both pairs] Speckle (left) is reduced (right) by the deformable mirror.

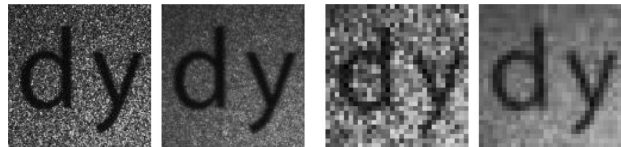


Fig. 2. [Left pair] Regions of a 2D hologram image focused onto a screen. [Right pair] The same image observed with the same camera and lens $f/\#$ but from a further distance. [Both pairs] Speckle (left) is reduced (right) by the deformable mirror.

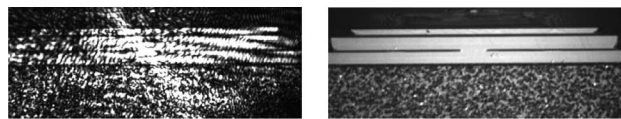


Fig. 3. Magneto-optical Kerr microscope image of a magnetic storage disc recording head. Illumination from a 445 nm laser diode, scale 1 $\mu\text{m}/20$ pixels, exposure period 1 ms. Inhomogeneous distribution of intensity (left) is improved (right) by the deformable mirror.

on a commercially available, mixed-signal, system-on-a-chip integrated circuit (IC), is used to generate highly randomized distributions of deformations.

3. RESULTS

Performance and other benefits are presented in the following sections, with particular comparison to moving diffusers.

A. Optical Efficiency

Intensity measurements made within the illumination optical system of a projection display, and at the screen, are over 50%

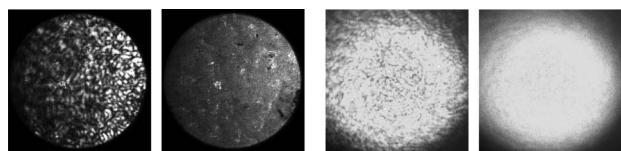


Fig. 4. [Left pair] Exit face of 105 μm diameter, 0.22 NA, multi-mode fiber of 3 m length. Light from a 532 nm laser source was coupled into entrance face via deformable mirror in inactive and active states. [Right pair] Regions on a screen at 1 m distance illuminated through the same fiber. [Both pairs] Inhomogeneous distribution of intensity (left) is improved (right) by the deformable mirror.

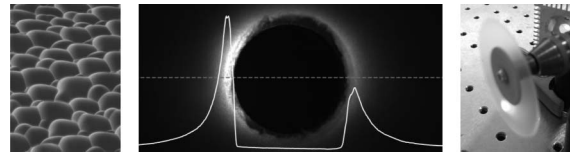


Fig. 5. [Left] Surface structure of an RPC Photonics Inc. engineered diffuser. Although it is smooth piecewise, its slopes are discontinuous such that diffraction occurs. [Center] Aperture of a beam trap positioned to accept laser light diverged approx. 6 deg by a cascade of two RPC EDS2 diffusers (one rotating.) The plot of mean intensity in the neighborhood of the center line shows losses. [Right] EDS2 diffuser rotated by an electric motor with incident laser light diffused.

higher for a deformable mirror than for a cascade of two diffusers; see Figs. 9 and 10 and [2] for further details.

B. Speed

Observations made with single and multiple 1 μs laser pulses are shown in Fig. 11. Speckle contrast ratio measurements are listed Table 1. It was impractical to build a rotating diffuser apparatus for comparison because the speed required for equivalent performance would be >100 m/s. See [3,4] for further details. Note that a customer has reported good speckle reduction with a single 100 ns laser pulse [private correspondence].

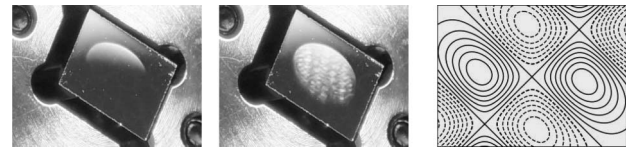


Fig. 6. [Left pair] Small deformable mirror in inactive and active states. Elliptical central region of 3 mm \times 4.5 mm is actuated at hundreds of kHz to excite randomly distributed surface deformations for angular divergence without diffraction losses. Reflection efficiency is approx. 99% and damage threshold is approx. 6 W. Power consumption depends on application requirements but is typically ≤ 100 mW. [Right] Contour plot of simulated surface wave heights showing smooth transitions between regions of convex and concave curvatures. As heights change over time the curvature of each region is reversed such that directions of reflection are changed.



Fig. 7. [Left] Typical deformable mirror configuration for illumination. Light from one or more laser sources is directed into a 10 mm² area, for example. Reflected light can be directed into a larger area with a smaller angle or vice versa, in accordance with the optical invariant. [Right pair] Regions illuminated using the same deformable mirror actuated for different surface wave amplitudes such that divergence angles are approx. 2 deg and 3 deg, respectively. No light is scattered outside these regions.

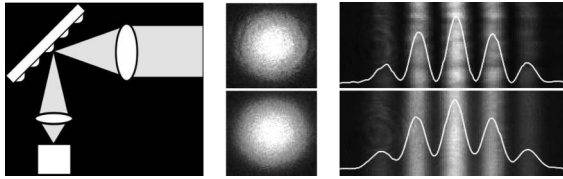


Fig. 8. [Left] Typical deformable mirror configuration for (pseudo-)collimation. Light from a laser source is focused into a spot of 0.01 mm^2 area, for example. [Center pair] Diameter of the beam increases proportional to additional divergence when the deformable is mirror active (below) versus inactive (above.) [Right pair] Interference fringes from double-slit apparatus with $300 \text{ }\mu\text{m}$ separation and 532 nm laser source with 0.2 nm spectral linewidth. Contrast is reduced proportional to the spot size when the deformable mirror is active (below) versus inactive (above.)

C. Size

Figure 12 shows deformable mirrors of different sizes that have been developed for various applications. Further details are provided in [5,6]. Although high optical powers can be handled conveniently by distribution over a large surface area, smaller areas are preferred in optical design. Therefore, we have prioritized the development of small devices with high reflectivity.



Fig. 9. Exit face of homogenizing and shaping rod of dimensions $6 \text{ mm} \times 8 \text{ mm} \times 50 \text{ mm}$ located after the deformable mirror in an illumination optical system with a 445 nm laser diode. [Left] With one stationary and one rotating EDS2 diffuser. [Center] With one rotating EDS2 diffuser only, mean intensity is 21% higher than with two diffusers. Homogeneity is not as good due to an effect relating to diffuser structure. [Right] With deformable mirror only, mean intensity is 57% higher than with two diffusers. To emphasize that there was no diffuser in the system, for the acquisition of this image the deformable mirror was controlled so as *not* to achieve good homogeneity.

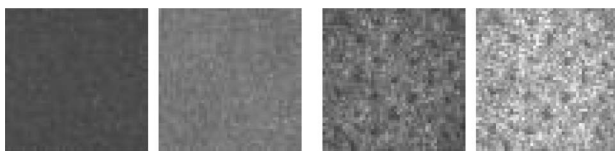


Fig. 10. Regions of the exit face shown in Fig. 9 projected by an $f/2.4$ lens and with $150\times$ magnification. [Left pair] Low-gain matte painted surface. Speckle contrast ratios both approx. 6%. [Right pair] High-gain rough metallic surface of polarization-preserving 3D cinema screen (with holes for sound transmission). Speckle contrast ratios both approx. 16%. [Both pairs] The relative improvement mean of intensity between the two diffusers (left) and deformable mirror (right) configurations is approx. equal to those measured at the exit face, as shown in Fig. 9.

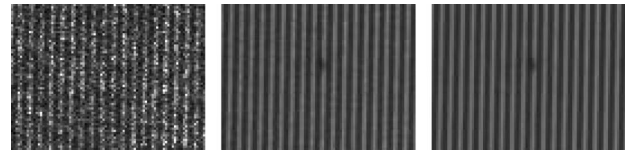


Fig. 11. Glass slide with striped pattern illuminated by a 445 nm laser diode through a Köhler optical system. [Left] Speckle from a single $1 \text{ }\mu\text{s}$ pulse. [Center] Speckle from a single $1 \text{ }\mu\text{s}$ pulse reduced by the deformable mirror. [Right] Average of 25 single $1 \text{ }\mu\text{s}$ pulses with speckle reduced by the deformable mirror.

Table 1. Speckle Contrast Ratios from the Apparatus Described in Fig. 11 for Different Numbers of Single $1 \text{ }\mu\text{s}$ Pulses with Deformable Mirror Inactive and Active^a

Pulse(s)	DM Inactive (%)	DM Active (%)
1	40.7	5.5
4	40.6	4.0
9	40.6	3.3
16	40.6	3.0
25	40.6	2.8

^aFor multiple pulses the multiple images were averaged before calculating the ratio. Note that a sequence of mutually incoherent pulses does *not* generate a sequence of uncorrelated speckle patterns.

D. Reliability

The only moving parts are piezoelectric actuators and sensors rated by their manufacturers for 100,000 h lifetimes, and the surface of the deformable mirror. We have not undertaken accelerated lifetime testing, but we do have devices active for over 50,000 h without failure. Our understanding is that the amplitude of surface motion is within the elastic limit of the material such that mechanical fatigue does not arise, as with MEMS resonators.

E. Wavelengths

Figure 1 shows effective speckle reduction at deep ultraviolet and long infrared wavelengths with different mirror coatings and different actuators and control electronics for the much higher surface wave deformation amplitudes required for the infrared.



Fig. 12. [Left] Small deformable mirror of active area dimensions $3.0 \text{ mm} \times 4.5 \text{ mm}$ with all control electronics fully integrated into its mounting PCB. [Center] Large deformable mirror of active area dimensions $40 \text{ mm} \times 50 \text{ mm}$ with control electronics mounted externally. Evaluated for projection display applications with $>100 \text{ W}$ optical power at visible wavelengths. [Right] Small deformable mirror with approx. 99% reflectivity dichroic stack coating optimized for certain red, green, and blue wavelengths, reflecting 6 W of CW optical power from a 445 nm laser diode distributed over an approx. $4.5 \text{ mm} \times 0.5 \text{ mm}$ area.

4. DISCUSSION

Our technology has been used in optical systems of many kinds, including those for display, sensing, microscopy, interferometry, spectroscopy, and holography, for applications as diverse as directional lighting and the detection of exoplanets.

A. Display

Many microdisplay-based projection display manufacturers have adopted lasers for a variety of reasons including low étendue for efficient transmission through systems that have as low as 10% optical efficiency with conventional sources. Deformable mirror performance can be seen in Fig. 13 and has been reported elsewhere, including [6–10].

Some direct-view displays have LEDs located at the edges of the light-guide plate used to distribute illumination over the panel. At least one manufacturer uses red laser diodes, coupled through optical fiber to the edge of the plate, to improve color quality [11]. Deformable mirror performance for such a configuration can be seen in Fig. 14 and has been reported in [12].

Another approach for improvement of color quality is to use quantum dot material for wavelength downconversion of blue from LEDs. An alternative is to use blue laser diodes instead, with a deformable mirror to improve homogeneity of distribution across the quantum dot material and to reduce speckle in the transmitted blue, as has been reported in [13].

Holographic displays are used in certain automotive head-up display systems and are being investigated for augmented and virtual reality applications. Speckle reduction with conventional techniques is challenging since preservation of coherence is necessary for image formation. However, the deformable mirror is effective, as can be seen in Fig. 15 and discussed in [14].

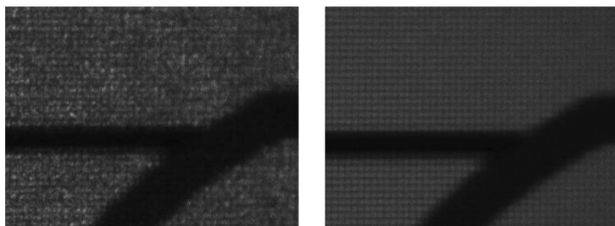


Fig. 13. Regions of an image formed by a Texas Instruments Inc. DLP projection display with illumination optical system modified to include the deformable mirror and to accept light from an external 532 nm laser source. Speckle (left) is reduced (right) by deformable mirror.

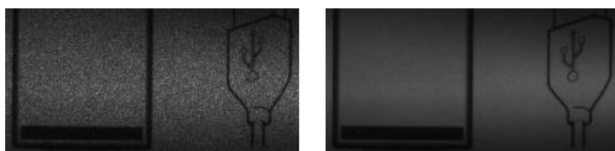


Fig. 14. Regions from an Amazon Kindle Paperwhite front-lit display modified with multimode fiber butt-coupled to the edge of its light guide plate. Light from external 532 nm laser source coupled into fiber via deformable mirror. Speckle (left) is significantly reduced (right) by the deformable mirror.

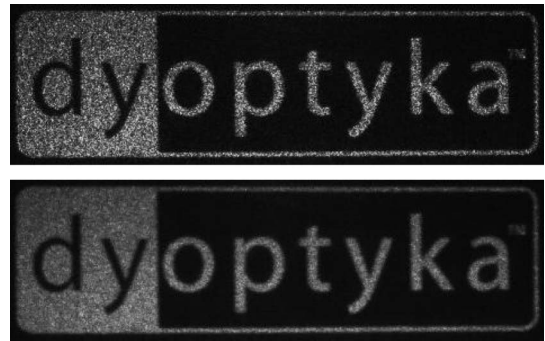


Fig. 15. Hologram image formed by Jasper Display Corp. LCoS microdisplay with 1920×1080 pixel phase modulation. Additional views of same image are provided in Fig. 2. Speckle (top) is reduced (bottom) by deformable mirror in (pseudo-)collimation configuration shown in Fig. 8.

Scanned beam laser displays are a challenging application because beam quality must be preserved, and the flying spot pixel display period can be very short, 15 ns for example. An approach using the deformable mirror is reported in [15]. Further work is ongoing, motivated in part by the popularity of technically similar LIDAR systems for automotive applications.

B. Microscopy

Deformable mirror performance in different types of microscopes can be seen in Figs. 1 and 3; also in Fig. 4 since optical fiber and light guides with small entrance apertures are often used. Details of some systems have been reported; see [16,17], for example.

C. Lighting

Highly directional “white light” illumination systems using phosphor for wavelength downconversion from blue laser diodes, are commercially available as automotive headlights. Problems include heating and cracking of phosphor due

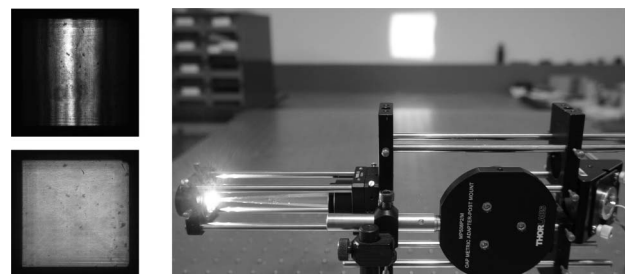


Fig. 16. [Left pair] Light from a 445 nm multimode laser diode at the $1 \text{ mm} \times 1 \text{ mm}$ face of a tapered glass light guide, having entered through the larger face. Inhomogeneous distribution of intensity (above) is improved (below) by the deformable mirror. [Right] Apparatus for directional white light illumination. From left to right: $1 \text{ mm} \times 1 \text{ mm} \times 1 \text{ mm}$ single-crystal Ce:YAG phosphor downconverting incident blue to yellow; tapered glass light guide for reduction of divergence; off-axis parabolic reflector with small hole for transmission of incident blue; enclosure for deformable mirror and 6 W blue laser diode. Far: Highly defined area of illumination perceived as white, comprising an emitted yellow and reflected blue.

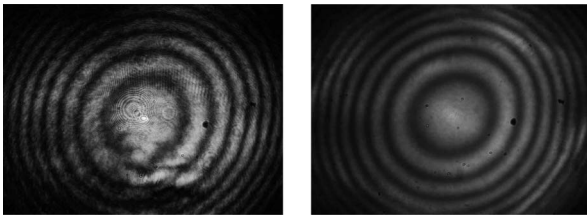


Fig. 17. Interference fringes from a beam profile reflectometry microscope. Unwanted interference effects (left) are reduced (right) by the deformable mirror located in common path before separation of arms. Note that contrast of fringes is reduced but smoothness is improved, which facilitates analysis.

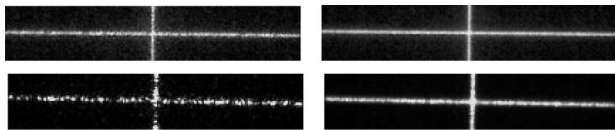


Fig. 18. [Top pair] Crosshair pattern on relatively smooth paper screen formed by HOLOEYE Photonics AG diffractive optical element. [Bottom pair] Same pattern formed by the same element on rougher diffusing screen results in worse interference effects. [Both pairs] Inhomogeneity and speckle (left) are reduced (right) by the deformable mirror.

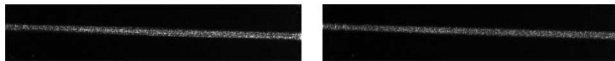


Fig. 19. Exit face of 105 μm diameter, 0.22 NA multimode fiber focused in one dimension only by cylindrical lens to form a line of width approx. 125 μm on a relatively smooth anodized metal surface. Inhomogeneity and speckle (left) are reduced (right) by the deformable mirror.

to inhomogeneous distribution of the intense incident illumination, poor color balance also due to inhomogeneous distribution, and speckle in the transmitted blue. Details of how the deformable mirror is used to address these problems are reported in [18,19]. A prototype system is described in Fig. 16.

D. Metrology

Figure 17 shows typical good performance in an interferometer and similar performance is reported in [20]. An additional benefit for this application is that a short laser pulse can be used to minimize the effects of vibration that may arise during the sensor integration period.

Lasers are often used for line and pattern projection in “structured light” three-dimensional metrology systems. Performance with a pattern-forming diffractive optical element is shown in Fig. 18 and with a line-forming cylindrical lens in Fig. 19.

5. CONCLUSIONS

Dyoptyka’s innovative deformable mirror technology offers a unique combination of advantages over moving diffusers,

including optical efficiency of speckle reduction, speed, size, and reliability.

REFERENCES

1. J. Goodman, *Speckle Phenomena in Optics* (Roberts and Company, 2007).
2. F. Shevlin, “Optically efficient homogenization of laser illumination,” in *International Display Workshop* (Institute of Image Information and Television Engineers, Society for Information Display, 2015).
3. F. Shevlin, “Speckle reduction within a single one microsecond laser pulse,” in *International Display Workshop* (Institute of Image Information and Television Engineers, Society for Information Display, 2012).
4. F. Shevlin, “Speckle reduction with multiple laser pulses,” in *2nd Laser Display Conference* (Optical Society of Japan, Japan Society of Applied Physics, 2013).
5. F. Shevlin, “A compact, low cost, phase randomizing device for laser illuminated displays,” in *International Display Workshop* (Institute of Image Information and Television Engineers, Society for Information Display, 2014).
6. F. Shevlin, “Speckle reduction in laser-illuminated pico-projectors,” *Proc. SPIE* **8252**, 825206 (2012).
7. H.-A. Chen, J.-W. Pan, and Z.-P. Yang, “Speckle reduction using deformable mirrors with diffusers in a laser pico-projector,” *Opt. Express* **25**, 18140–18151 (2017).
8. T.-T.-K. Tran, X. Chen, Ø. Svensen, and M. N. Akram, “Speckle reduction in laser projection using a dynamic deformable mirror,” *Opt. Express* **22**, 11152–11166 (2014).
9. T.-K.-T. Tran, Ø. Svensen, X. Chen, and M. N. Akram, “Speckle reduction in laser projection displays through angle and wavelength diversity,” *Appl. Opt.* **55**, 1267–1274 (2016).
10. F. Shevlin, “Speckle mitigation in laser-based projectors,” in *First Laser Display Conference* (Optical Society of Japan, The Japan Society of Applied Physics, 2012).
11. N. Nakano, E. Niikura, R. Murase, A. Nagase, T. Sasagawa, K. Minami, and M. Hanai, “Development of the backlight using laser light source for LCD,” in *2nd Laser Display Conference* (Optical Society of Japan, The Japan Society of Applied Physics, 2013).
12. F. Shevlin, “Light guide plate illumination by laser through optical fiber,” in *3rd Laser Display Conference* (Optical Society of Japan, The Japan Society of Applied Physics, 2014).
13. F. Shevlin, “Light guide plate illumination with blue laser and quantum dot emission,” in *International Display Workshop* (Institute of Image Information and Television Engineers, Society for Information Display, 2014).
14. F. Shevlin, “Dynamic illumination for spatio-temporal integration of unwanted interference in holographic displays,” in *7th Laser Display and Lighting Conference* (Optical Society of Japan, The Japan Society of Applied Physics, 2018).
15. F. Shevlin, “Beam quality-preserving speckle reduction for scanned laser displays,” in *4th Laser Display and Lighting Conference* (Optical Society of Japan, The Japan Society of Applied Physics, 2015).
16. M. Lequime, L. Abel-Tibérini, J. Lumeau, K. Gasc, and J. Berthon, “Complex pixellated optical filters,” in *International Conference on Space Optics* (2014).
17. V. Studer, J. Bobin, M. Chahid, H. S. Mousavi, E. Candes, and M. Dahan, “Compressive fluorescence microscopy for biological and hyperspectral imaging,” *Proc. Natl. Acad. Sci. U. S. A.* **109**, E1679–E1687 (2012).
18. F. Shevlin, “Speckle reduction for illumination with lasers and stationary, heat sinked, phosphors,” in *International Display Workshop* (Institute of Image Information and Television Engineers, Society for Information Display, 2013).
19. F. Shevlin, “Optically efficient directional illumination with homogenization of laser incidence on remote phosphor,” in *5th Laser Display and Lighting Conference* (Optical Society of Japan, The Japan Society of Applied Physics, 2016).
20. M. Frade, J. M. Enguita, and I. Álvarez, “In-situ waviness characterization of metal plates by a lateral shearing interferometric profilometer,” *Sensors* **13**, 4906–4921 (2013).